Task 2A Report: Pile Impactor and Restraint Design

Evaluation of Glass Fiber Reinforced Polymer (GFRP) Spirals in Corrosion Resistant Concrete Piles

FDOT Contract Number: BDV30 977-27, FSU Project ID: 042924

Progress report date: 8/7/2019

(Initial submission to FDOT Structures Research Center: 5/28/2019; First revision: 7/15/2019)

Submitted to:

Florida Department of Transportation

Research Center

605 Suwannee Street

Tallahassee, Florida 32399-0450

Project Managers:

Christina Freeman	FDOT Structures Research Center
Ge Wan	FDOT Structures Design Office
Rodrigo Herrera	FDOT Structures Design Office

Prepared by:

Olayiwola Adegbulugbe	Graduate Research Assistant
Sungmoon Jung	Principal Investigator
Raphael Kampmann	Co-Principal Investigator

Department of Civil and Environmental Engineering

FAMU-FSU College of Engineering

2525 Pottsdamer St., Tallahassee, FL. 32310.

Chapter 2. Impactor and Restraint Design

2.1 Design Requirements

2.1.1 Summary of Hammer Specifications and FDOT Pendulum Facility

The previous progress report (Task 1) had a detailed review of pile hammer types, specifications, and FDOT pendulum facility. Specifications relevant to the impactor design are as follows. The impact velocity of the hammer ranged between about 5 ft/sec to 30 ft/sec. The rated energy had a wide range (about 5 kip-ft to over 2000 kip-ft), but for typical hammers the rated energy was about 70 kip-ft to 120 kip-ft.

In this task, the experimental apparatus will be designed to simulate the impact loading of the pile driving system based on the specifications shown above. The apparatus will be constructed as an addition to the impact testing facility at and by the FDOT Structures Research Center, and therefore, is bound by the capabilities of the current pendulum facility. The pendulum has the capacity to swing an impact mass of up to 9020 lb. (4090 kg) through a drop height of 35 ft. The FDOT pendulum can deliver impact rated energy up to approximately 315 kip-ft. The length, width and depth of the reinforced concrete foundation for the anchor system are 34 ft, 20 ft and 3 ft respectively.

2.1.2 Design Requirements and Preferences

In addition to simulating typical pile driving hammer impact velocity and energy, the apparatus should be able to apply the compressive stress limit on the concrete pile. The maximum allowed pile stresses are given in the Florida DOT Standard Specifications 455-5.12.2 (FDOT, 2018). The maximum allowed pile compressive stress for concrete pile is given as:

$$s_{apc} = 0.7f_c' - 0.75f_{pe} \qquad (2.1)$$

where:

f_c' = specified minimum compressive strength of concrete (psi)

f_{pe}= effective prestress (after all losses) at the time of driving (psi), taken as 0.8 times the initial prestress force.

For typical production piles, assuming $f_c' = 6000$ psi and the initial prestress before losses is 1000 psi, the maximum allowable compressive stress (s_{apc}) is calculated as s_{apc} = [0.7(6000 psi) – 0.75(0.8 × 1000 psi)] / 1000 = 3.6 ksi. Depending on the properties of piles driven in the field, the maximum compressive stress measured during driving can be larger than this number. For example, based on the measured compressive strength $f_c' = 10000$ and design $f_{pe} = 1000$, s_{apc} was 6.25 ksi for the 24 in. square CFRP prestressed concrete pile used in the Deer Crossing Bridge project (Roddenberry et al. 2014). As explained in Task 1 report, the pile toe stress can be up to twice the pile top stress for the rigid support condition. Therefore, if the pile top stress reaches 5 ksi, the apparatus should be able to deliver approximately 10 ksi at the pile toe.

Design requirements for the impactor and the pile restraint can be summarized as follows:

- Impact velocity = approximately 5 ft/sec to 30 ft/sec
- Impact energy = approximately 70 kip-ft to 120 kip-ft
- Pile top stress = 5 ksi

The first two requirements are only for the impactor, whereas the third requirement (pile top stress) depends on both the impactor and the pile restraint design. The pile restraint also should be designed while considering the ease of the testing. Design preferences are as follows:

- Lower impactor height is preferred
- Displacement of the restraining block should not be excessive
- Minimum or no use of soil is preferred

The first preference is because the lower height makes it easier to control the impactor during the testing. If the displacement of the restraining block is excessive, it needs to be moved after each impact, which can increase the testing time. Similarly, use of soil will require much longer time to prepare the testing.

2.2 Design Concepts

The first design concept is shown in Figure 2.1, whereby the support-restraining structure is bolted to the strong floor to prevent movement of the pile. The pile would be placed on top of the frame structure, so the pile is free to slide but constrained by the end plate. Essentially, the pile will be under fixed-end support condition that can produce the large stress in the pile toe. In this design

approach, most of the potential energy will be transferred to the pile and subsequently to the support frame after the impact. Therefore, a smaller mass can be used for the impactor. This design concept was presented to the FDOT project managers. A concern was raised that this design may damage the bolt holes in the strong floor. The project team discarded the first design concept and developed another design concept.

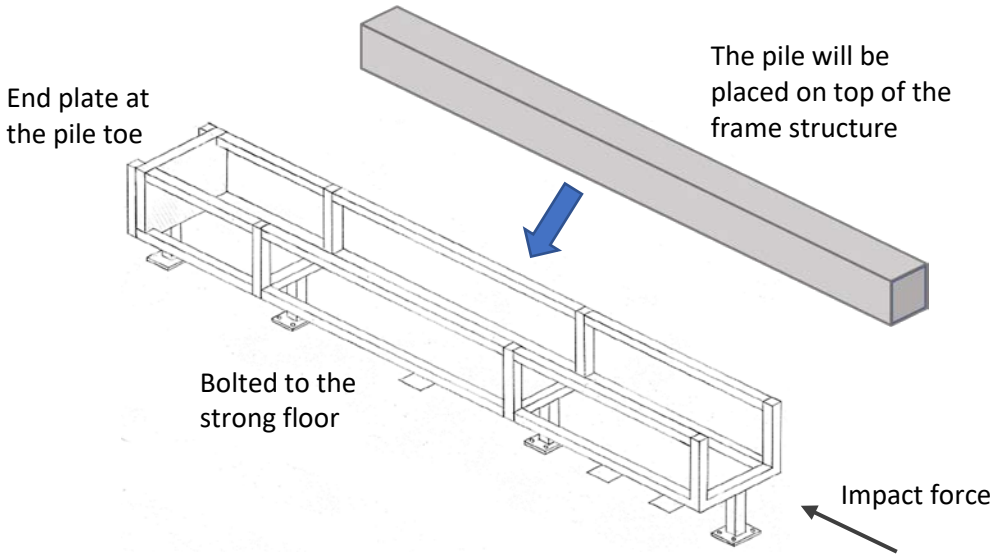

Figure 2.1: Illustration of the rigid-support design

In the second design concept shown in Figure 2.2, the pile specimen is placed on top of the roller support (or a similar mechanism) that does not constrain the movement of the pile along the direction of the impact force. Although this condition is different from an actual pile installation that penetrates through the soil, it does not have energy loss on the side of the pile. Therefore, a smaller impactor mass can produce the required pile top stress, which is the objective of the experiment. The objective of the experiment does not include simulation of the actual soil condition, which not only is difficult to reproduce but also greatly increase the time to conduct the experiment.

In this design, multiple blocks are placed adjacent to the pile toe. The pile and the blocks will slide after the impact. Therefore, the potential energy of the impactor will be converted to the kinetic energy of the pile and the blocks. The blocks will come to rest due to the friction between the

blocks and the ground. In the rest of the report, design calculations and drawings for the second design concept will be presented.

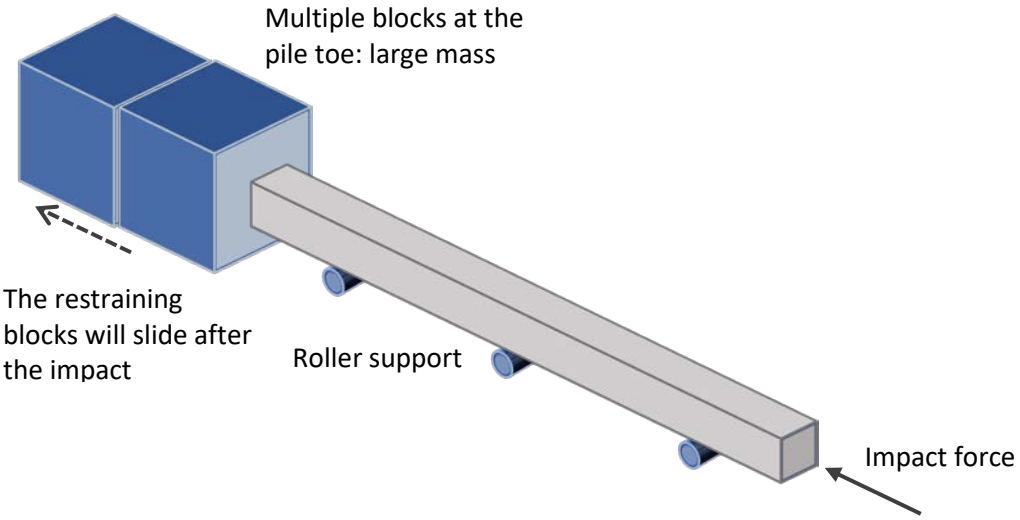

Figure 2.2: Illustration of the block-based design

2.3 Design Calculations

2.3.1 Background

Analytical equations and finite element analyses were used to design the impactor and the pile restraint. The process was iterative, but only the final calculations will be shown below for concise presentation. The objective was to ensure that design requirements can be met for certain drop height, without damaging the experimental apparatus.

During the actual experiment, gradually increasing drop height will be used in order to obtain more data for the same specimen. Since the prediction of the impact stress is highly uncertain, gradually increasing the drop height will ensure that the behavior of the pile before and after the failure can be studied. Major sources of uncertainties are friction between the pile restraint and the soil, and plywood insert at the pile top and pile toe. However, the impact stress can be easily adjusted during the experiment by increasing or decreasing the drop height. In the design, we selected the target drop height such that it can be easily increased or decreased, rather than using very low or very high drop height that are difficult to adjust.

2.3.2 Analytical Calculation

Suppose the mass of the impactor is m_a, the drop height is h, and the velocity of the impactor immediately before hitting the pile (after the drop) is v_{ai}. Since energy loss due to the swing of the impactor is negligible, the impact energy can be determined from the potential energy of the impactor:

$$E_p = m_a g h \tag{2.2}$$

The kinetic energy, immediately before the impact, is:

$$E_k = \frac{1}{2} m_a v_{ai}^2 \tag{2.3}$$

The impact velocity for various drop heights can be found by equating E_p and E_k. With an impactor of mass 5511 lbm (2500 kg), Figure 2.3 plots the impact velocity and the impact energy of the impactor for various drop heights. The maximum drop height of the FDOT pendulum facility is 35 ft. The impactor is expected to achieve the target impact velocity of 30 ft/sec at 14 ft drop height. At this height, the impact energy is 77 kip-ft, which is within the target range between 70 kip-ft and 120 kip-ft. If needed, the impact energy of 120 kip-ft can be reached by increasing the drop height to 22 ft.

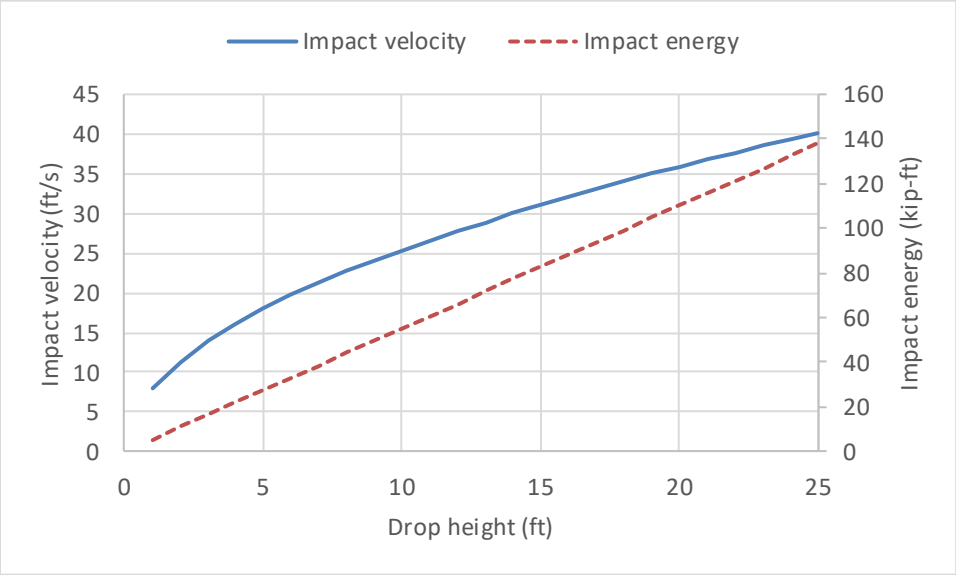

Figure 2.3: Impact velocity and impact energy of the impactor

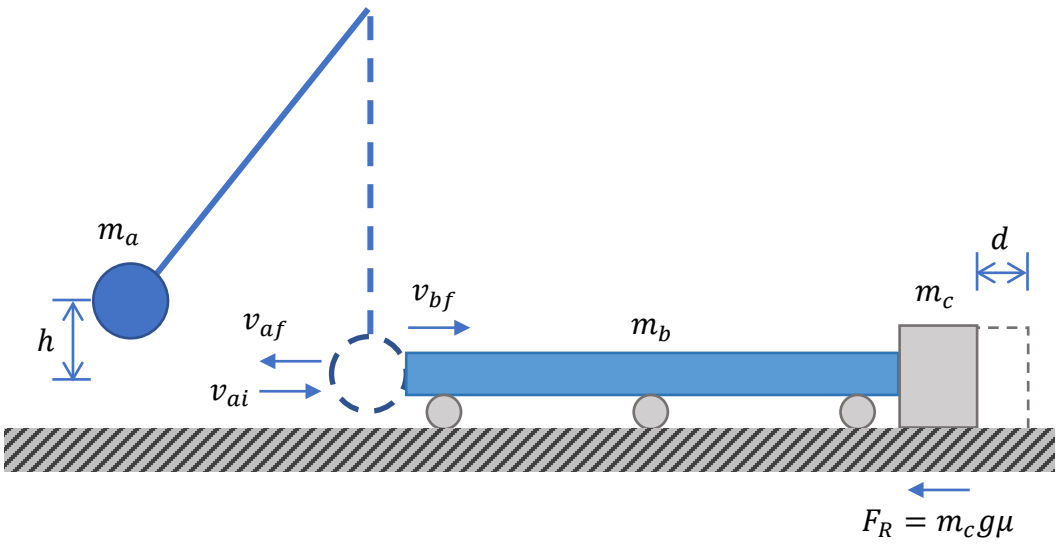

Figure 2.4: Schematic diagram of the impactor and the pile restraint

Let us now introduce variables necessary for further discussions. Figure 2.4 shows a schematic diagram of the impactor and the pile restraint, where d is the displacement of the pile restraining blocks after the impact. m_b and m_c are the mass of the pile and pile restraining blocks, respectively. v_{ai}, v_{af}, $v_{bi} = 0$, and v_{bf} are the velocity of the impactor just before the impact, velocity of the impactor after the impact, velocity of the pile restraint before the impact, and velocity of the pile restraint after the impact, respectively. The friction between the pile restraints and the soil depends on m_c, gravity g, and friction coefficient μ. Finally, the coefficient of restitution C_R is assumed to be 0.5. This number must be obtained experimentally, but it can also be estimated from the finite element analysis, which was done in this report.

The objective of the following analysis was twofold: to understand the physics in order to better design the impactor and the pile restraint, and to come up with rough estimates necessary for the finite element analysis. In this simple analytical calculation, an isolated system was assumed. Again, although the process was iterative, only the most relevant scenarios will be discussed. A more accurate estimation can be found in the finite element analysis.

Let us follow the directions of the velocities shown in Figure 2.4. From conservation of momentum:

$$m_a v_{ai} = (m_b + m_c) v_{bf} - m_a v_{af} \tag{2.4}$$

From the definition of the coefficient of restitution:

$$C_R = \frac{v_{bf} + v_{af}}{v_{ai}} \tag{2.5}$$

Once the masses are determined from the design process, v_{af} and v_{bf} can be found from equations (2.4) and (2.5). The mass of the pile m_b was assumed to be 8165 kg (18,000 lbs) using the concrete pile dimension of 2 ft × 2 ft × 30 ft. m_a and m_c were chosen from the design process.

The main design requirement is to be able to exert 5 ksi stress at the pile top. For the 2 ft × 2 ft pile cross-section, the corresponding force is 2880 kips. Accurate calculation of the peak impact force is not possible analytically, but an average impact force can be estimated from the impulse-momentum theorem:

$$F_{avg} t = (m_b + m_c) v_{bf} \tag{2.6}$$

A rough estimate of the impact time t is to use the one-quarter of the sign-wave, i.e., the response of the pile under the impulse F_{avg}. Here, it is assumed that the impactor bounces backwards after reaching the peak displacement (compression) of the pile. The pile is assumed to be an axial "spring." Then, the impact time is:

$$t = \frac{T_n}{4} = \left(\frac{2\pi}{\omega_n}\right)\left(\frac{1}{4}\right) \tag{2.7}$$

By solving the partial differential equation of an axially loaded member, the natural frequency can be obtained as:

$$\omega_n = \frac{\pi}{2L}\sqrt{\frac{EA}{m_b/L}} \tag{2.8}$$

where, L is the length of the pile. Based on the previous research (Roddenberry et al. 2014), $E = 6178$ ksi was used. The corresponding $t = 0.00217$ seconds. Note that this is not the time of peak stress (which cannot be obtained analytically), but the impact time to estimate the average impact force.

As discussed earlier, the target impact velocity of 30 ft/sec can be reached at 14 ft drop height. Impact force was estimated for this drop height. During the design, the restraint mass m_c between 22,046 lbm (10,000 kg) and 88,184 lbm (40,000 kg) was considered. The average impact force F_{avg} was estimated to be between 3121 kips and 3375 kips. Therefore, the required 5 ksi stress can be applied to the pile top. Given that the drop height can be increased to further increase the impact energy if needed, the analytical analysis confirmed that the design goal can be met.

The F_{avg} is a very rough estimate, because the effect of the slide and the plywood commonly used in pile installation were not included in this analysis. These will decrease the impact force. On the other hand, this force is an average force, and the peak impact force will be much larger. A more accurate estimate will be given in the finite element analysis.

Finally, the displacement of the restraints can be estimated from the conservation of energy:

$$\frac{1}{2}(m_b + m_c)v_{bf}^2 = F_R d \qquad (2.9)$$

The friction force F_R depends on the friction coefficient μ. One of the design preferences is to minimize the displacement of the restraining blocks. Excessive displacement of the restraining blocks will significantly increase the time to conduct the experiment, because of the need to move the blocks with a crane even after an impact from a low drop height. Figure 2.5 shows estimated movement of the restraining blocks obtained by using the earlier equations and equation (2.9). A 6 in. deep gravel subgrade would be provided below the designed steel-concrete restraining blocks, while subsequent blocks will be placed on the adjacent soil. Based on the friction that can be obtained between concrete and soil, μ is assumed as 0.45.

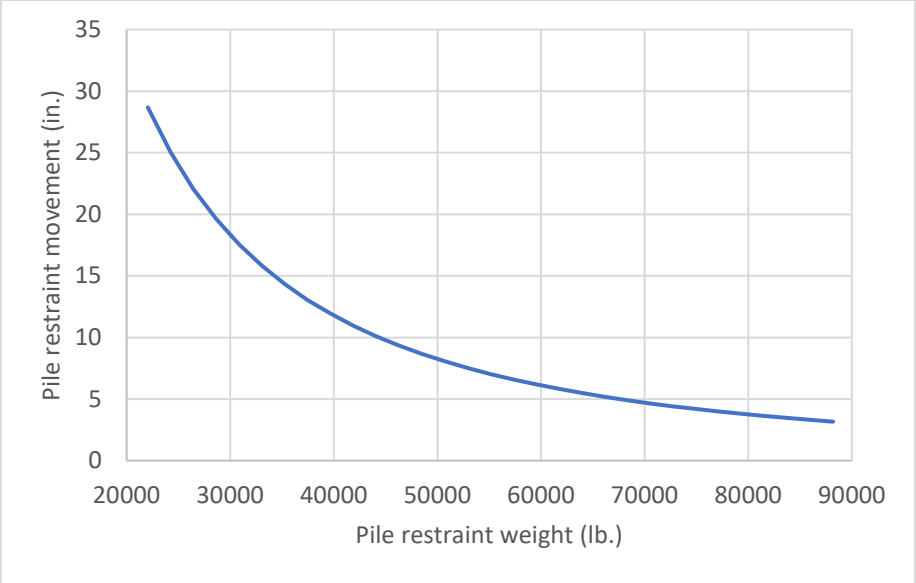

Figure 2.5: Estimated movement of the restraining blocks

Two 4 ft × 4 ft × 6 ft steel blocks made of 0.75-inch-thick plates, filled with concrete, were designed to restrain the pile. Detailed drawings are attached with the report. The mass of each block is estimated to be 16,900 lb. (7,666 kg). In addition, FDOT has concrete blocks with the dimension 8 ft × 7 ft × 3 ft that were constructed for UHPC splice testing. The mass of these blocks was estimated as 25,200 lb. (11,431 kg) each. By using two 4 ft × 4 ft × 6 ft steel-concrete blocks and one 8 ft × 7 ft × 3 ft concrete block, the total mass of the support was chosen as 59,000 lbm (26,762 kg). Based on the analytical calculations, the displacement of the restraining block was estimated to be 6.3 inch. This design was chosen as the main design in the finite element analyses. One more scenario was also analyzed in the finite element analysis, in order to find out how much the displacement could be reduced. In the second scenario, six restraining blocks – two 4 ft × 4 ft × 6 ft steel-concrete blocks and four 8 ft × 7 ft × 3 ft concrete blocks – were used with a combined mass of 134,600 lb. (61,053 kg). Based on the analytical calculations for the second scenario, the displacement of the restraining block was estimated to be 1.5 inch.

2.3.3 Finite Element Analyses

Finite element analyses were used throughout the design process. This section will discuss the finite element analysis results for the three-block and six-block restraint scenarios described initially. The SI units were used in the finite element analysis. Parameters presented in this section

will primarily be in SI units, however, U.S. customary units are provided in parenthesis as needed. Figure 2.6 shows the components of the impact tests that were simulated by the LS-Dyna software for the three-block restraint scenario. The explicit finite element solver was used to analyze the impact test.

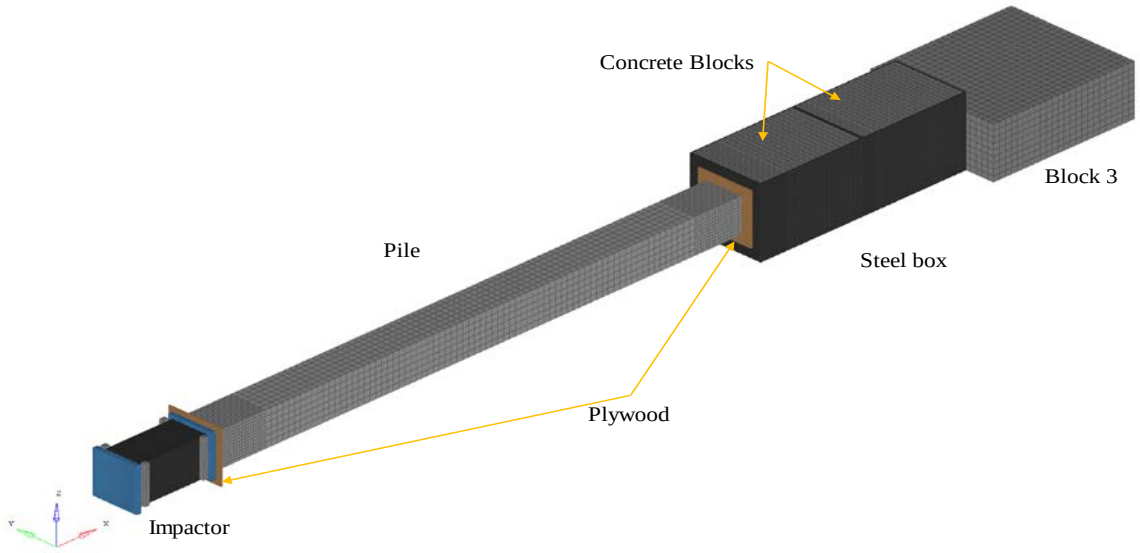

Figure 2.6: Modeling the pile impact in LS-Dyna

As for the elements, the 3D solid element with full integration formulation (ELEFORM 2) were used to model all the parts. Beam element (1D) was used to define the welding connections between the steel parts. The concrete pile was modelled with the fine mesh size at both ends and coarse mesh for the middle part. Two sheets of 3/4 inch-thick (19 mm) plywood were also added at two contact points between the pile with the impactor and with the restraining blocks. Two different contact algorithms “node to surface” and “automatic single surface” were utilized between different parts of the model.

All the steel components were modelled using piecewise linear plasticity (Isotropic MAT 24). The steel was assumed to become perfectly plastic at 500 MPa. The effect of strain rate was considered by using viscoplastic formulation (VP=1) (Škrlec and Klemenc, 2016). To save the computational time, the elastic material model was used for the concrete since detailed failure analysis of the concrete was not the goal of this task, and the main design parameters were the shapes and dimensions of the steel parts (Murray, 2007a). In addition, most of the concrete elements stayed

within the yield stress limit. To simulate the failure mechanism in the plywood, the MAT_143 WOOD with 10% moisture was used (Murray, 2007b; Otkur, 2010). Table 2.1 shows the details of the FE model. Table 2.2 shows material properties of each component.

Table 2.1: Summary of FE model

Component	Material	Total mass (Kg)	Element size (min, max) (mm)
Impactor	Steel (elastic-plastic)	2520 (5556 lb.)	10, 20 (0.4 in.,0.8 in.)
Pile	Concrete (elastic)	8257 (18204 lb.)	100 (4 in.)
Steel box	Steel (elastic-plastic)	1350 (2976 lb.)	5, 20 (0.2 in., 0.8 in.)
Concrete Block	Concrete (elastic)	7481 (16493 lb.)	25 (1 in)
Plywood	Wood (elastic-plastic)	21 (46 lb.)	5 (0.2 in.)
UHPC Block	Concrete (elastic)	11793 (25999 lb.)	100 (4 in.)

Table 2.2: Material properties used in the analysis

Material	Density (kg/m3)	Module of Elasticity (GPa)	Yield stress (MPa)	Poisson's ratio
Steel (impactor)	7850 (490 lb./ft.^{3})	210 (3×10^4 ksi)	350 (50.7 ksi)	0.3
Steel (blocks)	7850 (490 lb./ft.^{3})	210 (3×10^4 ksi)	250 (36.2 ksi)	0.3
Concrete (pile)	2430(151 lb./ft.^{3})	42.5 (6.1×10^3 ksi)	70 (50.7 ksi)	0.3
Concrete (blocks)	2400(150 lb./ft.^{3})	26.3 (3.8×10^3 ksi)	50 (10.1 ksi)	0.3
Wood	673(42 lb./ft.^{3})	E_L =16.7 (2.4×10^3 ksi) (Longitudinal) E_T= 0.1 (14.5 ksi) (Transverse)	42 (6 ksi) (tensile) 54 (7.8 ksi) (compressive)	0.15

The boundary conditions were defined such that only the movement along the direction of the impact (x-direction) was allowed. The coefficient of friction between the three blocks and ground

was assumed as 0.45. Time step of 0.0001 seconds was chosen for the output files. The analysis was continued up to 0.6 seconds when the displacement of the restraining blocks showed convergence.

2.3.3.1 Finite Element Analyses – Three-Block Restraint Scenario

In section 2.3.2, it was shown that the impactor is expected to achieve the target impact velocity of 9.144 m/s (30 ft/sec) at 14 ft drop height. Analysis results for this case will be shown first. The simulation was conducted by applying 9.144 m/s initial velocity to the impactor part. Figure 2.7 shows the maximum von Mises stress for the impactor. The impactor will be fabricated with the grade 50 steel, and the yield stress is 350 MPa as shown in Table 2.2. In the contour plot, the colors orange and red are greater than the yield stress. The stresses in the impactor was well below the yield stress limit for this case. Also, the concrete stress behind the 3 in. plate of the impactor showed a maximum stress of 25 MPa (3.6 ksi).

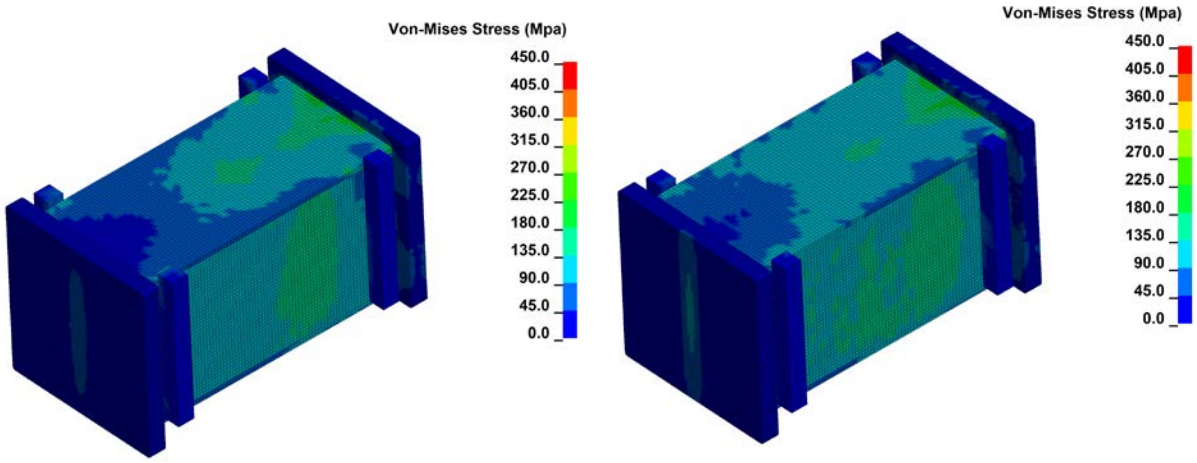

Figure 2.7: Von Mises stress for the impactor test (V=9.14 m/s (30 ft/sec)) during the t=0.0024s & 0.0025s

For the pile restraint arrangement with three blocks, Figure 2.8 shows the von Mises stress at four different time steps for the front plate of the first restraint block, where the highest stresses were observed. This plate is the first contact point between the pile and the restraining blocks. To save costs, Grade 36 steel plates would be used to construct the steel-concrete restraining blocks. Lime (green-yellow) to red colors in Figure 2.8 show regions with stress greater than the yield stress of 250 MPa. Although some regions exceeded the yield stress, these stresses were observed on the

surface for a fraction of a second (t ≅ 0.0001s) and are not likely to cause significant permanent deformation.

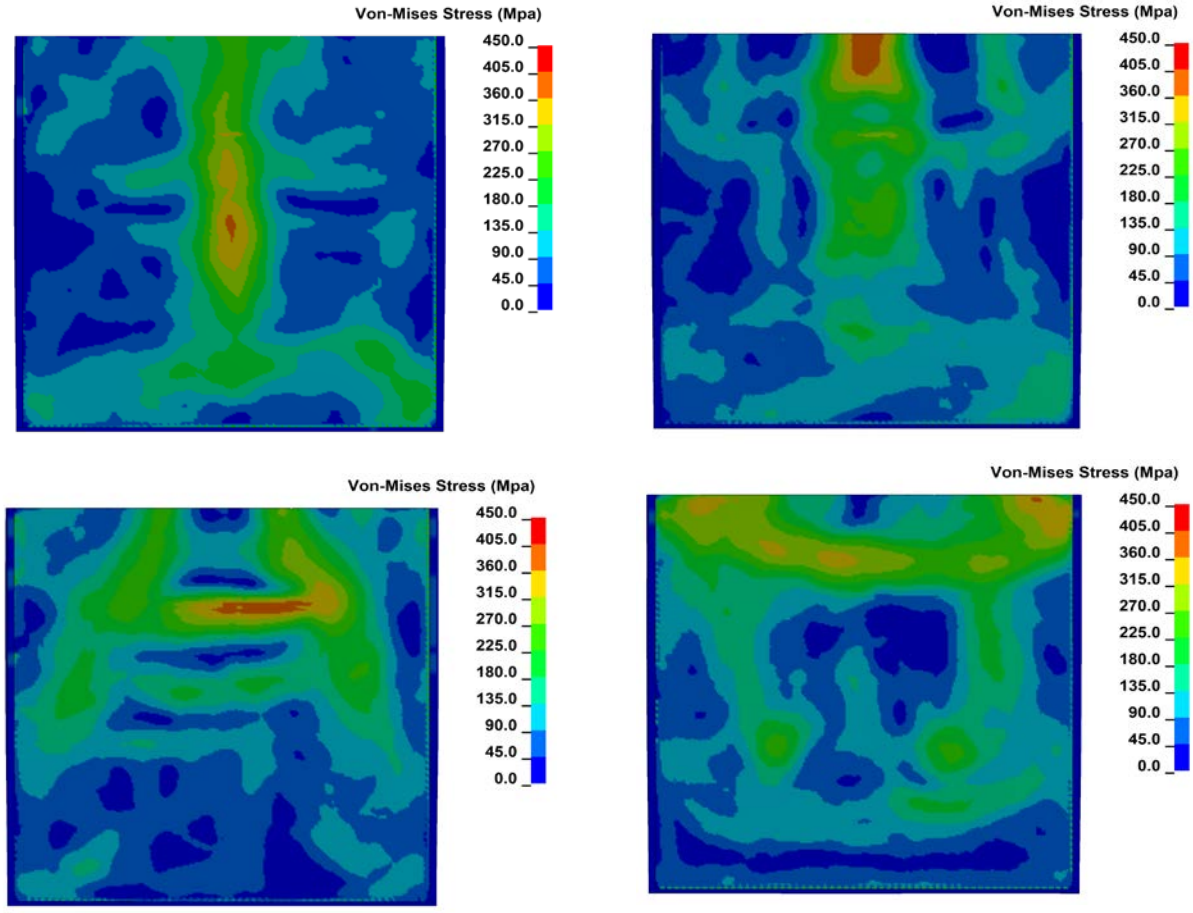

Figure 2.8: Von Mises stress for the front plate of the pile restraint (V=9.14 m/s (30 ft/sec); for four different time steps that showed the largest stresses)

The plastic deformation (permanent deformation) and failure mechanism of the steel plate highly depend on the material parameters. To obtain the accurate mechanical behavior of the steel plate at high strain rate it is necessary to identify the strain rate characteristics of the steel plate using either experimental or theoretical method. For the current simulation, the strain-stress curve which was extracted from quasi-static test on mild steel hollow section was used. Figure 2.9 shows the plastic strain resulted for the base simulation with the impact velocity of 9.14 m/s (30 ft/s). The plastic strain values were significantly small (ε_{max}=0.002). As a result, since the size of the element

in plate is 5 mm (0.2 in.), the maximum permanent deformation would be less than 1 mm (0.04 in.) which can be negligible for this test.

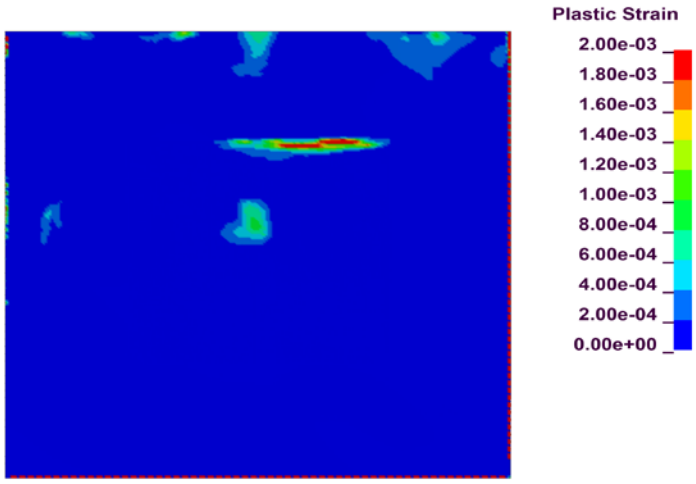

Figure 2.9: Permanent plastic strain of the frontal plate in first block

Figure 2.10 shows the von Mises and axial (x-direction) stress for the front and end section of the concrete pile. For each section, the time step when the maximum stress was observed was chosen. The larger stresses were observed at the end of the pile as expected. It should be noted that the concrete was assumed as an elastic material, and therefore, the results may change if a more sophisticated material model is used. However, this analysis still approximately predicts the stress exerted on the pile. The target stress at the pile top was 5 ksi (34.5 MPa), which was observed in the finite element analysis.

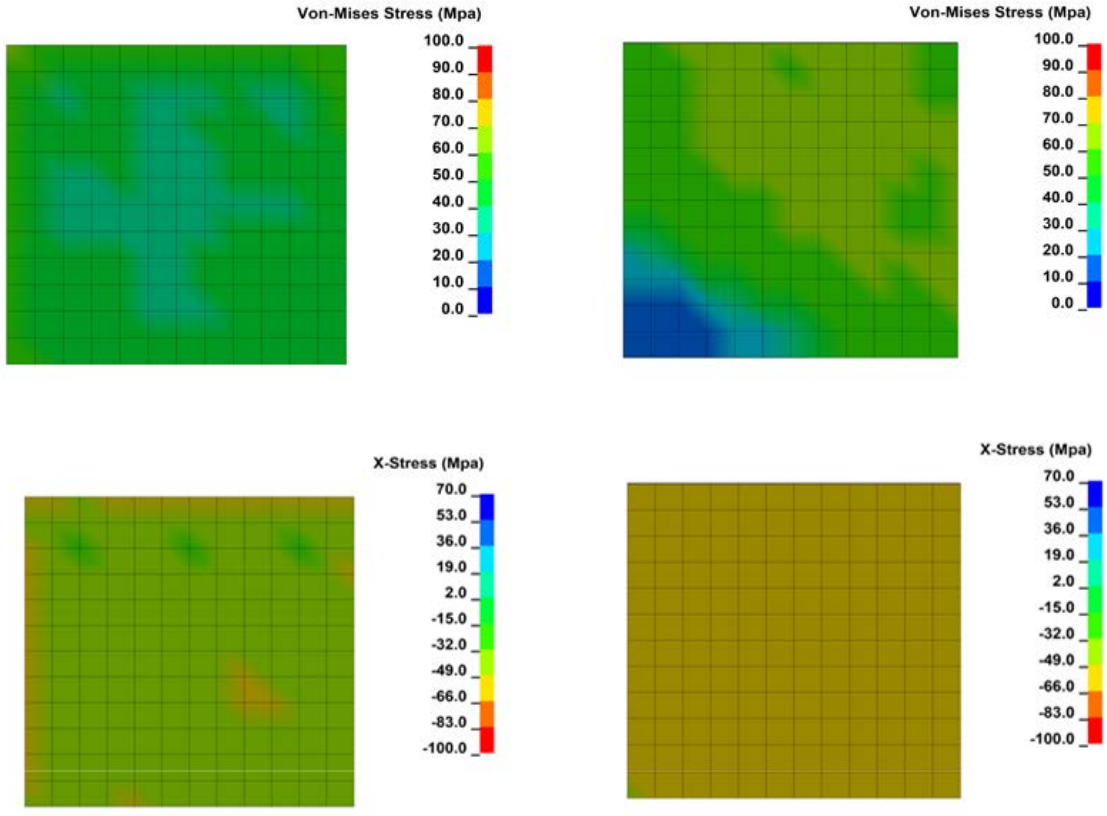

Figure 2.10: Maximum von Mises and x-stress at the beginning and end of the concrete pile (V=9.14 m/s (30 ft/sec))

Finally, the displacement of the restraint was 204 mm (8 in.) for a single drop. The displacement from the analytic calculation was 160 mm (6.3 in.) for the same friction coefficient. The displacements were comparable, the difference was 22 %. Due to the high uncertainty in the friction assumption, this number should be interpreted as a rough guideline rather than a precise prediction.

2.3.3.2 Finite Element Analyses – Three-Block Restraint Scenario with Angle Impact

Given a maximum skew of 0.47° allowed by the lateral restraint provided by the pile support assembly, the results of the stress analysis for steel plate of the first restraining block is shown in Figure 2.11.

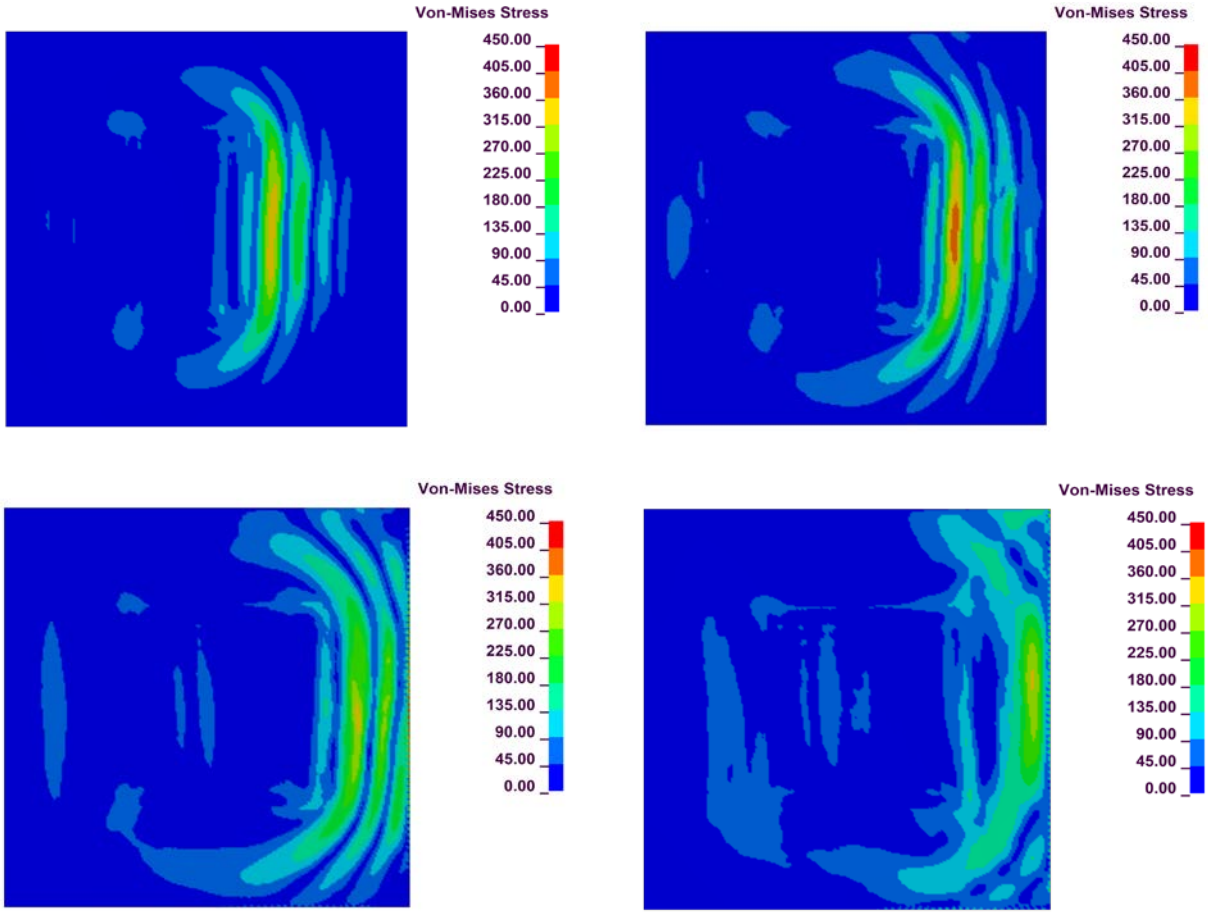

Figure 2.11: Stress distribution of the front plate in first block at different time step when the Corner of the pile struck the restraint

The plastic strain from this analysis shows that the maximum plastic deformation is less than 1 mm (0.04 in.) which is negligible. Figure 2.12 shows the area were the plastic deformation was observed.

Figure 2.13 shows the von Mises and axial (x-direction) stress for the front and end sections of the concrete pile.

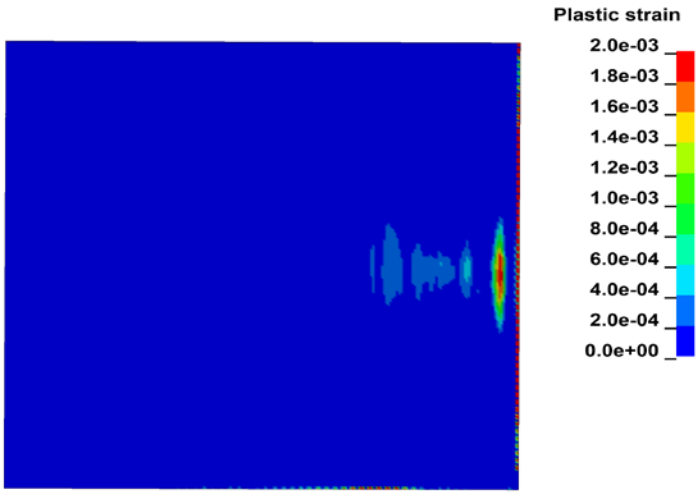

Figure 2.12: Permanent plastic strain of the front plate of first block (angle impact)

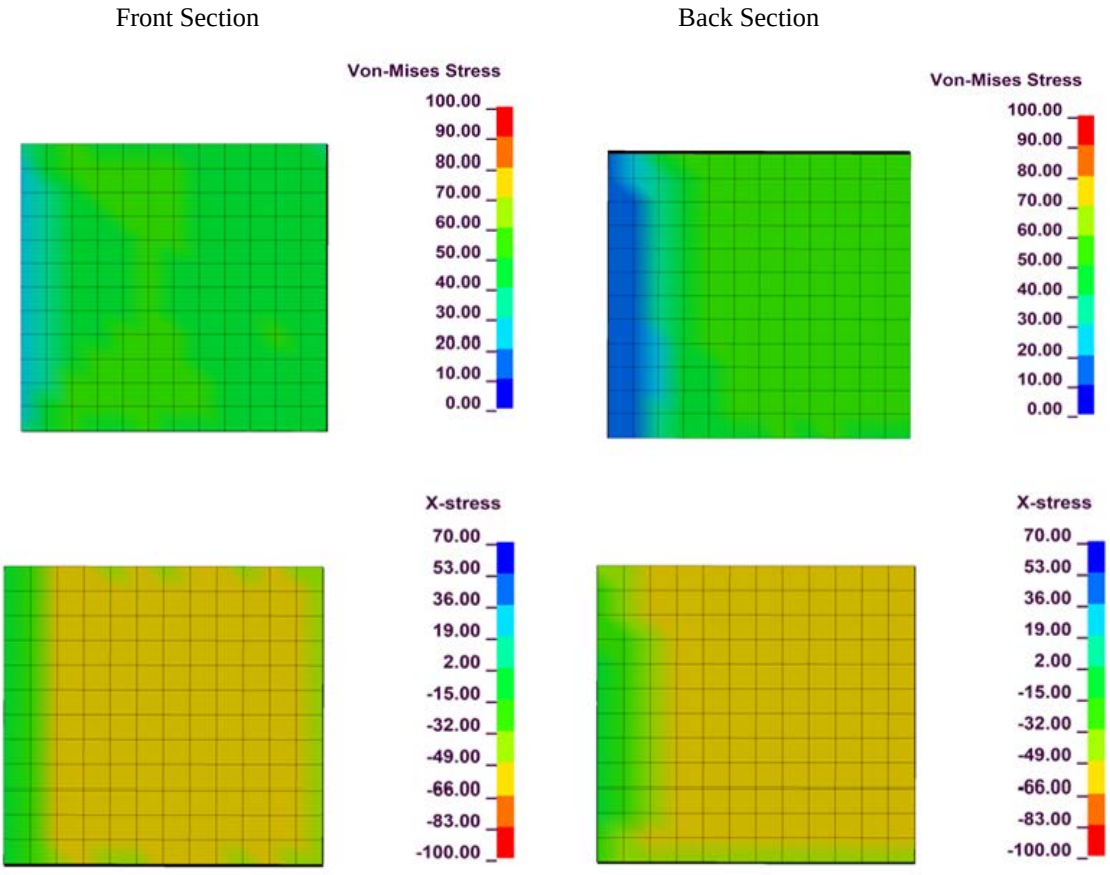

Figure 2.13: Maximum Von-mises and x-stress at the beginning and end of the concrete pile (angle impact with V=9.14m/s (30 ft/sec))

2.3.3.3 Finite Element Analyses – Six-Block Restraint Scenario

In this analysis, three more blocks were added to the pile restraint system. The position of the blocks is shown in Figure 2.14. The total displacement of each block converged to the constant value 0.3s after the impact whereas in previous analysis (three-block scenario) it took 0.6s for the blocks to reach their stationary position. Another difference was observed for the direction of movement for the first block. In current analysis – six-block scenario – it bounced back and moved – 24 mm (1 in.) relative to x direction, while in previous analysis – three-block scenario, it moved 90 mm along the x direction. Table 2.3 summarizes the results of the displacements of restraining blocks from the analyzed scenarios.

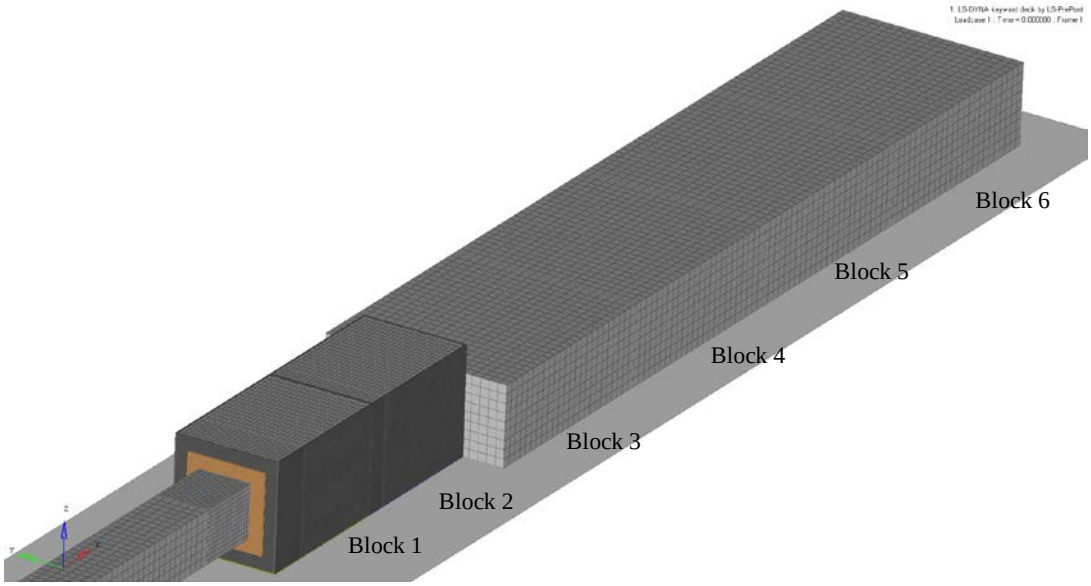

Figure 2.14: Pile restraint system and block numbering

Table 2.3: Summary of resulting displacements of restraining blocks from analytic and FEM analysis

Block No.	X-Displacement (mm)			
	3 Blocks analysis		6 Blocks analysis	
	Analytical	**FEM**	**Analytical**	**FEM**
Block 1	160 (6.3 in.)	90 (3.5 in.)	38 (1.5 in.)	-24 (1 in.)
Block 2	160 (6.3 in.)	165 (6.5 in.)	38 (1.5 in.)	5.6 (0.22 in.)
Block 3	160 (6.3 in.)	204 (8 in.)	38 (1.5 in.)	5.7 (0.22 in.)
Block 4	NA	NA	38 (1.5 in.)	8.8 (0.35 in.)
Block 5	NA	NA	38 (1.5 in.)	28 (1.1 in.)
Block 6	NA	NA	38 (1.5 in.)	245 (9.6 in.)

Figure 2.16 and Figure 2.15 show the stress distribution for the frontal plate of the first block the and the stress distribution at the front and back sections of the concrete pile respectively. Higher stress was observed for the analysis where three more blocks were added.

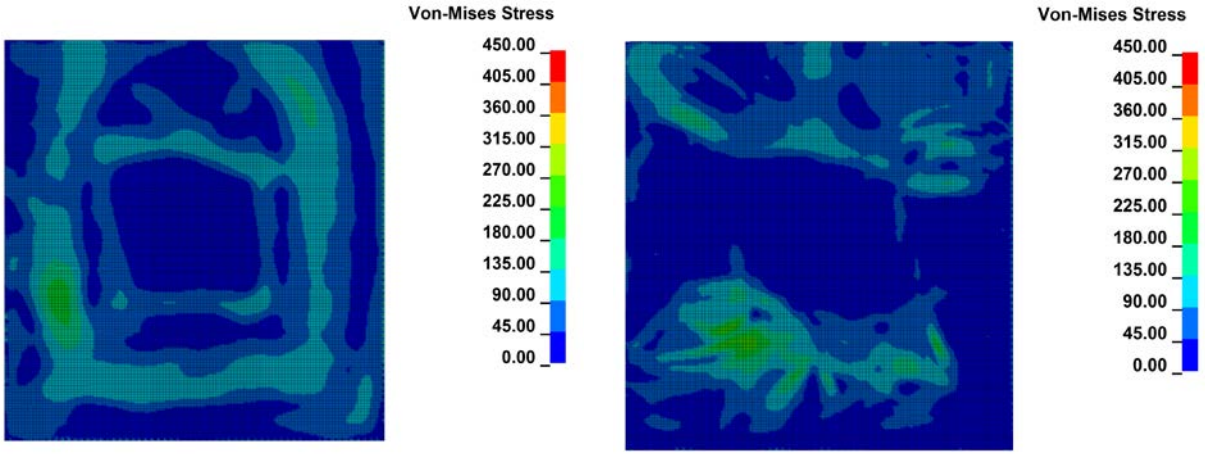

Figure 2.15: Maximum Von-mises stress distribution for the frontal plate of the first support (6 blocks analysis)

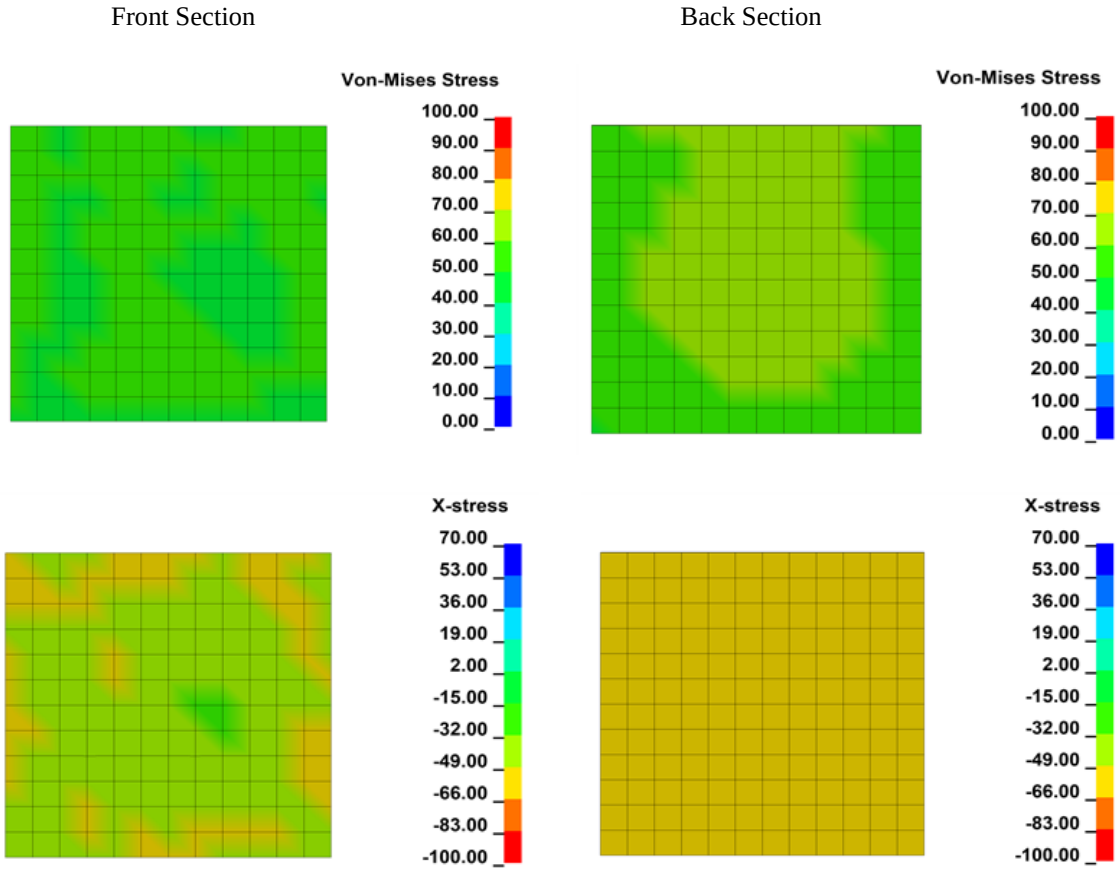

Figure 2.16: Maximum Von-mises and x-stress at the beginning and end of the concrete pile (6 blocks analysis with V=9.14m/s (30 ft/sec))

2.3.3.4 Finite Element Analyses for 22 ft. Drop Height Limit

The case discussed so far, 14 ft. drop height case, achieves the upper-bound of the impact velocity (30 ft/sec). The finite element analyses showed that the required impact stress was also achieved for the pile specimen. However, due to the uncertainties in the plywood modeling and friction assumptions, and any other potential issues not identified so far, there might be a need to adjust the drop height during the actual testing. In the following, the effects using a drop height of 22 ft. will be discussed. In this case, the impact energy of 120 kip-ft will be reached which is upper-bound of commonly used pile hammers. The corresponding impact velocity is 37.63 ft/sec (11.46 m/s).

As shown in Figure 2.17, the impactor was still within the yield stress, with an exception of the corners of the box where localized (less than one element – size 5mm) high stresses were observed.

For the front face of the pile restraint, larger areas compared to Figure 2.8 exceeded the yield stress. See Figure 2.18. However, as discussed earlier, these areas may not actually permanently deform and even if they do, the effect on the testing will be negligible. Figure 2.19 shows the stresses in the pile, which further exceeds the design requirements as expected.

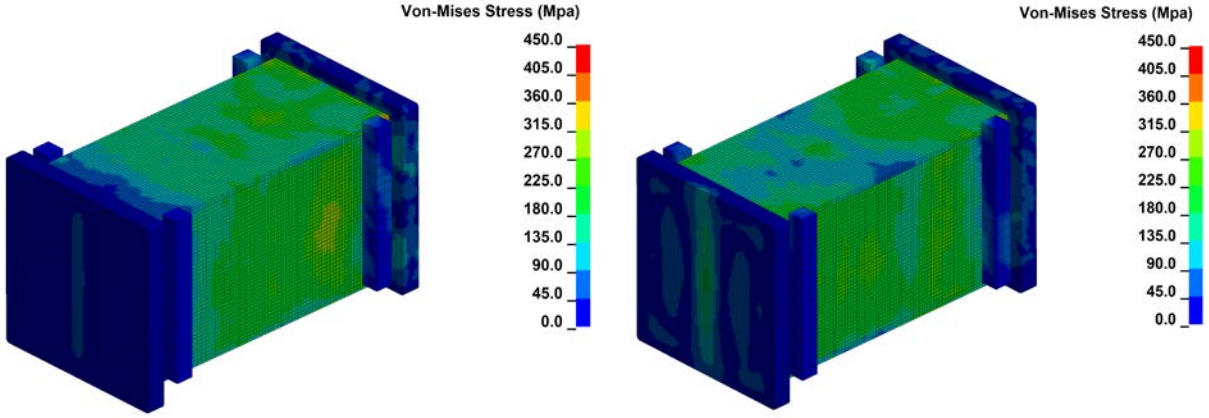

Figure 2.17: Von Mise stress for the impactor test (V=11.46 m/s (37.63 ft/sec)) for two different time steps

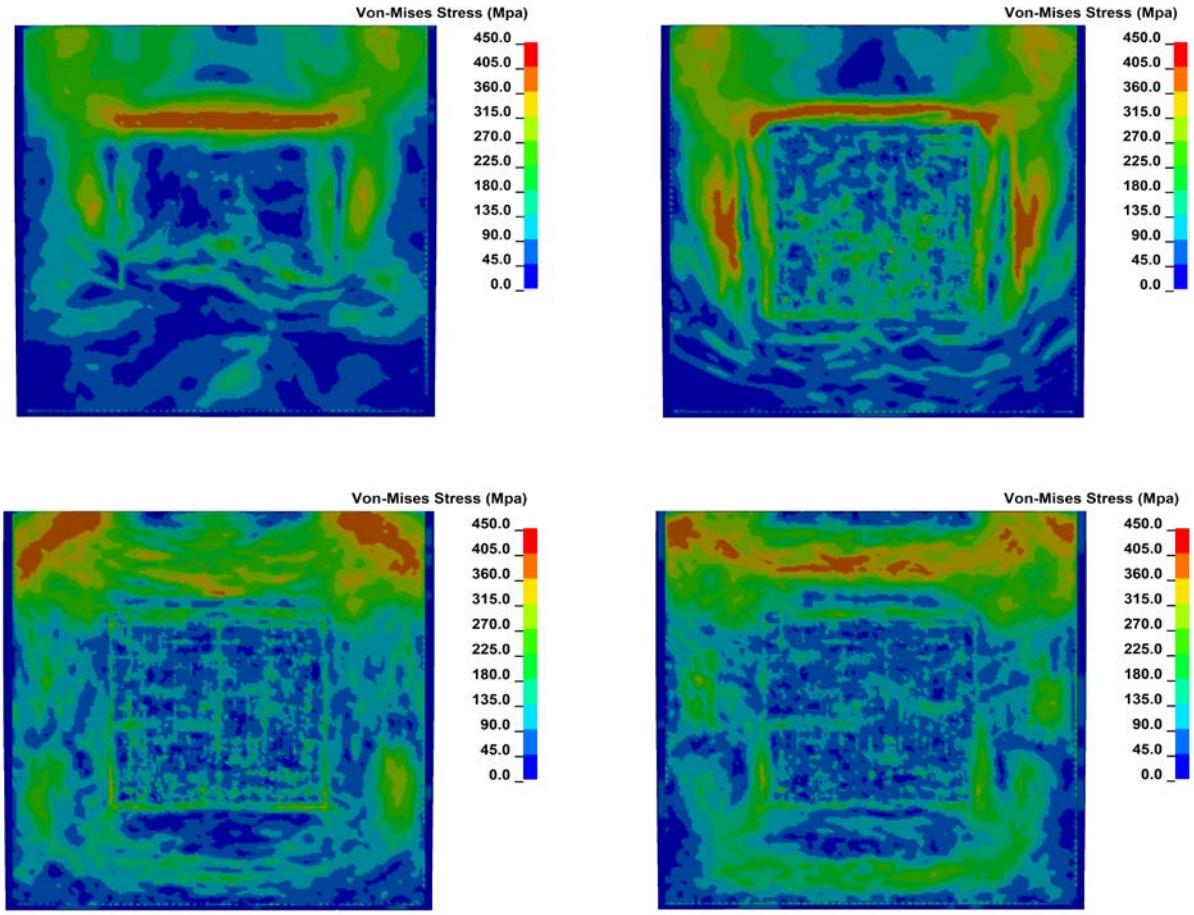

Figure 2.18: Von Mises stress for the front plate of the pile restraint (V=11.46 m/s (37.63 ft/sec); for four different time steps that showed the largest stresses)

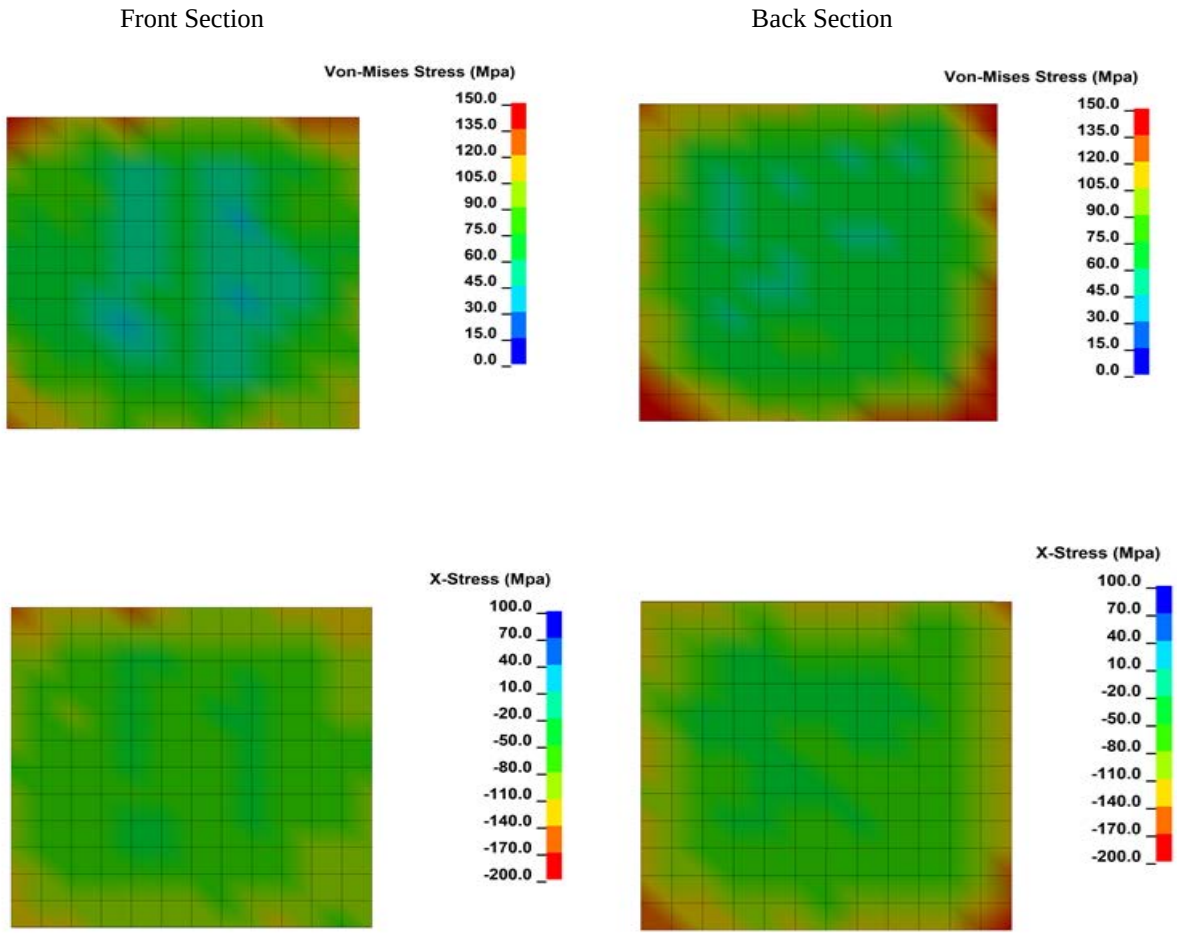

Figure 2.19: Maximum von Mises and x-stress at the beginning and end of the concrete pile (V=11.46 m/s (37.63 ft/sec))

2.4 Fabrication Drawings and Specifications

See the attached drawings.

Acknowledgement

Two members of the PI's research group participated in this task. Jeff Siervogel led the development of the impactor and pile restraint designs. Reza Seyedi conducted the finite element analyses and wrote a draft of section 2.3.3.

Bibliography

FDOT (2018). *FDOT Standard Specifications for Road and Bridge Construction*. Florida Department of Transportation, Tallahassee, FL.

Murray, Y.D. (2007a). Manual for LS-DYNA concrete material model 159. United States Federal Highway Administration, Turner-Fairbank Highway Research Center.

Murray, Y.D. (2007b). Manual for LS-DYNA wood material model 143. United States Federal Highway Administration, Turner-Fairbank Highway Research Center.

Otkur, M. (2010). Impact Modeling and Failure Modes of Composite Plywood. Texas Tech University.

Roddenberry, M., Mtenga, P., and Joshi, K. (2014). "Investigation of Carbon Fiber Composite Cables (CFCC) in Prestressed Concrete Piles," Florida Department of Transportation Final Report, BDK83-977-17.

Škrlec A., and Klemenc, J. (2016). "Estimating the Strain-Rate-Dependent Parameters of the Cowper-Symonds and Johnson-Cook Material Models using Taguchi Arrays," Journal of Mechanical Engineering, 62(4).